

Toward theoretically limited SPP propagation length above two hundred microns on ultra-smooth silver surface

ALEKSANDR S. BABURIN,^{1,2,7,*} ALEKSEY S. KALMYKOV,^{3,4,*}
 ROMAN V. KIRTAEV,⁵ DMITRIY V. NEGROV,⁵ DMITRIY O.
 MOSKALEV,¹ ILYA A. RYZHIKOV,^{1,6} PAVEL N. MELENTIEV,^{3,4,8} ILYA
 A. RODIONOV,^{1,2} AND VICTOR I. BALYKIN^{3,4,9}

¹Functional Micro/Nanosystems Research and Educational Center, Bauman Moscow State Technical University, 2nd Baumanskaya street 5, Moscow, 105005, Russian Federation

²Dukhov Research Institute of Automatics (VNIIA), Sushchevskaya street 22, Moscow 127055, Russian Federation

³Institute of Spectroscopy RAS, Troitsk, Moscow, 142190, Russia

⁴National Research University, Higher School of Economics, Moscow, 101000, Russia

⁵Moscow Institute of Physics and Technology, Dolgoprudny, 141700, Russia

⁶Institute for Theoretical and Applied Electromagnetics RAS, Izhorskaya street 13, Moscow, 125412, Russian Federation

⁷baburin@bmstu.ru

⁸melentiev@isan.troitsk.ru

⁹balykin@isan.troitsk.ru

*A.S. Baburin and A.S. Kalmykov are contributed equally to this work.

Abstract: We demonstrate the optical medium for surface plasmon - polariton waves (SPP) propagation with ultra low losses corresponding to the theoretically limited values. The unique element of the optical medium is an atomically-flat single-crystalline silver thin film which provides extremely low losses. The SPP excited on the surface of such thin films ($\lambda = 780$ nm) is characterized by a SPP propagation length equals to $200 \mu\text{m}$, which is twice longer than previously reported experimental results and corresponds to theoretically limited values for silver films.

© 2018 Optical Society of America under the terms of the [OSA Open Access Publishing Agreement](#)

OCIS codes: (240.6680) Surface plasmons; (250.5403) Plasmonics; (240.0310) Thin films.

1. J. B. Khurgin, How to deal with the loss in plasmonics and metamaterials, *Nat. nanotechnology* 10, 2 (2015).

2. V. I. Balykin and P. N. Melentiev, Optics and spectroscopy of individual plasmonic nanostructure, *Phys. Usp* (2017).

3. P. Melentiev, A. Kalmykov, A. Gritchenko, A. Afanasiev, V. Balykin, A. Baburin, E. Ryzhova, I. Filippov, I. Rodionov, I. Nechepurenko et al., Plasmonic nanolaser for intracavity spectroscopy and sensorics, *Appl. Phys. Lett.* 111, 213104 (2017).

4. J. Khurgin and G. Sun, Third-order nonlinear plasmonic materials: Enhancement and limitations, *Phys. Rev. A* 88, 053838 (2013).

5. G. Yankovskii, A. Komarov, R. Puzko, A. Baryshev, K. Afanasiev, I. Boginskaya, I. Bykov, A. Merzlikin, I. Rodionov, and I. Ryzhikov, Structural and optical properties of single and bilayer silver and gold films, *Phys. Solid State* 58, 2503-2510 (2016).

6. K. M. McPeak, S. V. Jayanti, S. J. Kress, S. Meyer, S. Iotti, A. Rossinelli, and D. J. Norris, Plasmonic films can easily be better: rules and recipes, *ACS photonics* 2, 326-333 (2015).

7. S. Kunwar, M. Sui, Q. Zhang, P. Pandey, M.-Y. Li, and J. Lee, Various silver nanostructures on sapphire using plasmon self-assembly and dewetting of thin films, *Nano-Micro Lett.* 9, 17 (2017).

8. A. S. Baburin, A. I. Ivanov, I. A. Ryzhikov, I. V. Trofimov, A. R. Gabidullin, D. O. Moskalev, Y. V. Panfilov, and I. A. Rodionov, Crystalline structure dependence on optical properties of silver thin film over time, in Progress In Electromagnetics Research Symposium-Spring (PIERS), 2017, (IEEE, 2017), pp. 1497-1502.
9. P. R. West, S. Ishii, G. V. Naik, N. K. Emani, V. M. Shalaev, and A. Boltasseva, Searching for better plasmonic materials, *Laser and Photonics Rev.* 4, 795-808 (2010).
10. J.-S. G. Bouillard, W. Dickson, D. P. O'Connor, G. A. Wurtz, and A. V. Zayats, Low-temperature plasmonics of metallic nanostructures, *Nano letters* 12, 1561-1565 (2012).
11. S. V. Jayanti, J. H. Park, A. Dejneka, D. Chvostova, K. M. McPeak, X. Chen, S.-H. Oh, and D. J. Norris, Low-temperature enhancement of plasmonic performance in silver films, *Opt. materials express* 5, 1147-1155 (2015).
12. H. Raether, Surface plasmons on smooth surfaces, in *Surface plasmons on smooth and rough surfaces and on gratings*, (Springer, 1988), pp. 4-39.
13. P. B. Johnson and R.-W. Christy, Optical constants of the noble metals, *Phys. review B* 6, 4370 (1972).
14. Y. Wu, C. Zhang, N. M. Estakhri, Y. Zhao, J. Kim, M. Zhang, X.-X. Liu, G. K. Pribil, A. AlÃ¡z, C.-K. Shih et al., Intrinsic optical properties and enhanced plasmonic response of epitaxial silver, *Adv. Mater.* 26, 6106-6110 (2014).
15. S. Babar and J. Weaver, Optical constants of Cu, Ag, and Au revisited, *Appl. Opt.* 54, 477-481 (2015).
16. P. Melentiev, A. A. Kuzin, and V. I. Balykin, Control of SPP propagation and focusing through scattering from nanostructures, *Quantum Electron.* 47, 266 (2017).
17. I. A. Rodionov, A. S. Baburin, A. V. Zverev, I. A. Philippov, A. R. Gabidulin, A. A. Dobronosova, E. V. Ryzhova, A. P. Vinogradov, A. I. Ivanov, S. S. Maklakov et al., Mass production compatible fabrication techniques of single-crystalline silver metamaterials and plasmonics devices, in *Metamaterials, Metadevices, and Metasystems 2017*, vol. 10343 (International Society for Optics and Photonics, 2017), vol. 10343, p. 1034337.
18. S. Bogdanov, M. Y. Shalaginov, A. Lagutchev, C.-C. Chiang, D. Shah, A. S. Baburin, I. A. Ryzhikov, I. A. Rodionov, A. Boltasseva, and V. M. Shalaev, Ultrabright room-temperature single-photon emission from nanodiamond nitrogen-vacancy centers with sub-nanosecond excited-state lifetime, arXiv preprint arXiv:1711.09481 (2017).
19. F. Lopez-Tejeira, S. G. Rodrigo, L. Martin-Moreno, F. J. Garcia-Vidal, E. Devaux, T. W. Ebbesen, J. R. Krenn, I. Radko, S. I. Bozhevolnyi, M. U. Gonzalez et al., Efficient unidirectional nanoslit couplers for surface plasmons, *Nat. Phys.* 3, 324 (2007).

1. Introduction

The important research area in nanoplasmonics is the propagation of plasmon waves on the surface of metal thin films. The practical applications of nanoplasmonics are strongly limited by the significant losses of SPP waves on metal surfaces [1-3]. The losses in metals inevitably limit the propagation length of the SPP wave, the Q factor of plasmonic resonators, and the cross section of optical nonlinear processes [4]. This problem is even worse in nanoplasmonics of the visible and near infrared spectral ranges.

There are many experimental researches demonstrating a strong difference for various metal films between measured SPP losses and calculated values even for well-known or measured optical constants [1,2]. Such a huge mismatch is the result of the metal thin films (crystalline structure, surface roughness, surface condition) and interfaces (substrate-metal, metal-media) imperfections. Single-crystalline metal thin films should be a proper way to solve described problems, but it is extremely hard to fabricate it with high quality. One of the most challenging metal in term of single-crystalline growth is silver, because of its natural chemical instability [5, 6]. High sensitivity to substrate surface reconstruction and impurities, lattice-matched substrate

dewetting at elevated growth temperatures [7] and optical properties degradation over time [8]. All the listed above silver film growth issues are in practice the potential sources of a its poor optical properties, characterized by a short SPP propagation length.

In the present work we demonstrate for the first time that properly synthesized atomically-flat single-crystalline silver thin film on silicon substrate (to be published) makes it possible to create the optical medium for surface plasmon - polariton waves (SPP) propagation with losses close to theoretically predicted values.

2. SPP propagation length on the silver film surface

The choice of material for creating a plasmonic nanostructures is decisive in achieving its best properties. Silver and gold are at the present time the main materials of experimental nanoplasmonics due to minimal ohmic losses among all known natural materials. However, these materials in the visible and ultraviolet regions of the spectrum exhibit significant ohmic losses. This leads to a practical impossibility to construct the nanoplasmonic devices with high quality parameters in these spectral ranges.

The ohmic losses in metals can be divided into two groups: (1) losses due to the presence of free conduction electrons and (2) losses due to bound electrons in metal. Losses from conduction electrons are due to electron-electron interaction, electron-phonon interaction, and due to scattering of electrons by lattice defects and grain boundaries in polycrystalline metals. Losses due to bound electrons arise when the photon is absorbed through the interband transition, with the electron transition to highly excited states. Both mechanisms of losses in metals strongly limit the progress in the development of nanoplasmonics.

Using silver one could obtain the minimal losses for SPP waves in the visible and near infrared regions of the spectrum [9]. A further reduction in losses can be achieved by cooling the material to cryogenic temperatures [10] with about 40-60% improvement in SPP propagation length was experimentally demonstrated by cooling the material down to cryogenic temperatures [11]. These results are consistent with the Drude-Lorentz model of the metal.

The SPP propagation length is the key parameter characterizing the plasmonic quality of metal films in term of future practical applications. The SPP propagation length is the length after which SPP wave intensity decreases to 1/e from its initial value [12]. The theoretical value of the SPP propagation length is determined by the optical constants of the silver (ϵ' - the real part, and ϵ'' - of the imaginary part of the dielectric permittivity of the silver film):

$$L_{SPP} = \frac{c}{\omega} \left(\frac{\epsilon' + 1}{\epsilon'} \right)^{3/2} \frac{(\epsilon')^2}{\epsilon''} \quad (1)$$

Thus, to calculate the SPP propagation length, it is necessary to know the dielectric constants of the silver film. There are numerous studies on silver films optical constants measured using spectroscopic ellipsometry. In the work [13], the optical constants were measured at wavelength of 780 nm that are $\epsilon' = -29.384$, $\epsilon'' = 0.365222$. The corresponding calculated SPP propagation length is 278 μm ($\lambda = 780$ nm). Another value of the SPP propagation length can be obtained by using the following data from [14]: $\epsilon' = -31.535$, $\epsilon'' = 0.4328$. The corresponding calculated the SPP propagation length equals to 271 μm ($\lambda = 780$ nm). The minimum calculated value of the SPP propagation length is obtained using the data of [15]: $\epsilon' = -29.688$, $\epsilon'' = 0.57674$, which corresponds to the SPP propagation length equal to 180 μm ($\lambda = 780$ nm). However, till the present, the largest experimentally measured SPP propagation length for silver nanofilms is about 100 μm at $\lambda = 780$ nm ($\lambda = 780$ nm)[16], which is several times less than the calculated values.

In all the experiments we used 100-nm-thick single-crystalline silver films [SCULL process, to be published] grown on a lattice-matched Si [111] substrates. The films were deposited by electron-beam evaporation (base pressure 3×10^{-8} Torr, 1 $\text{\AA}/\text{s}$ deposition rate) using 99.999%

silver pellets. The silver films demonstrate perfect optical properties combined with nanostructures patterning compatibility [17,18]. In this paper we present the SPP propagation length measurement results for such a single-crystalline silver thin films.

3. Measurement of the SPP propagation length on the surface of single-crystalline grown silver film

Measurement of the SPP propagation length is a rather complicated experimental problem and usually consists of two steps: (1) effective excitation of SPP wave and (2) measurement of the SPP propagation length. One of the most accessible, convincing and informative is the method of measuring the SPP propagation length based on registration of SPP wave which are excited by laser radiation. The SPP are excited by using a nanoslits array patterned on a metal film surface. Registration of the launched SPP is performed through the scattering the SPP on the nanogrooves (detectors of SPP waves) located on the metal film surface on the SPP propagation way Fig.1(c) [16].

We call this method "the far-field optical microscopy of SPP waves". In this method, the excitation of SPP is realized through the scattering of laser radiation on the array of nanoslits and the subsequent scattering of the launched SPP on nanogrooves. Detection of scattered radiation on nanogrooves in far field helps to visualize SPP propagation as well as to measure the SPP propagation length.

The measurements were made with silver films both on transparent [16], and on opaque substrates [14]. We note that optical microscopy of SPP waves on metallic films made on an opaque substrate is much more complicated in implementation, in comparison with the case of transparent substrates. This complexity is caused by the fact that excitation of the SPP and its detection is carried out from the same side of the substrate. In this case, the same microscope objective is used to excite SPP and then to detect radiation scattered by the SPP on nanostructures - detectors. The main problem here is to detect a weak scattering signal of SPP on the nanostructures - detectors against a giant reflected and scattered signals from a laser used to excite SPP.

Two types of nanostructures were created on the silver nanofilm surface using focused-ion-beam lithography. One of them was designed to excite SPP wave and was formed by a matrix of 20 slits nanostructures with a nanoslits spacing of $\Lambda_1 = 780$ nm and a slit size of $120 \text{ nm} \times 20 \mu\text{m}$. Another one served as a detector of the SPP wave, and was formed by a matrix of 15 nanogrooves with a depth of 40 nm and a size of $120 \text{ nm} \times 40 \mu\text{m}$ with a distance between nanogrooves equal to $20 \mu\text{m}$. Fig. 1(a,b) shows the electron microscope images of the created nanostructures.

Fig.1(c) shows the scheme for measuring the SPP propagation length. The measurements were performed using an inverted Nikon Eclipse/Ti-U microscope. To excite SPP wave, we used a CW semiconductor laser with a tunable wavelength around 780 nm, having ultra narrow linewidth. This laser light was focused with a microscope objective (x20) into a $6 \mu\text{m}$ spot on the array of nanoslits. The period of nanoslits array Λ_1 was chosen to effectively excite SPP on the film surface at orthogonal incidence of the laser beam on the sample [19]. The period was determined from the relation $Re(k_{SPP}) \approx G + k_0 \sin \alpha$, where k_{SPP} is the wave number of the SPP wave, $G = 2\pi/\Lambda_1$ is the modulus of the reciprocal lattice vector of the nanoslits array, α is the angle of laser radiation incidence on the sample ($\alpha = 90^\circ$), $k_0 = \omega c$ is the wavenumber of laser light.

We fabricated a series of parallel nanogrooves on the way of SPP propagation Fig.1(a). The radiation scattered on these nanogrooves is recorded with the same microscope objective lens on a 2D CCD camera (Princeton Instrument, PhotonMax). The radiation is proportional to the intensity of the SPP wave at the location of the nanogroove, and the detection of the scattered light from the array of nanogrooves allows us to measure the change of the SPP intensity during its propagation. To increase the contrast of the measured signal, we used two crossed polarizers with a residual extinction ratio of 1:1000. The first polarizer was installed in the laser beam, the second one - before the 2D CCD camera. In this case, the polarizations of the laser radiation and

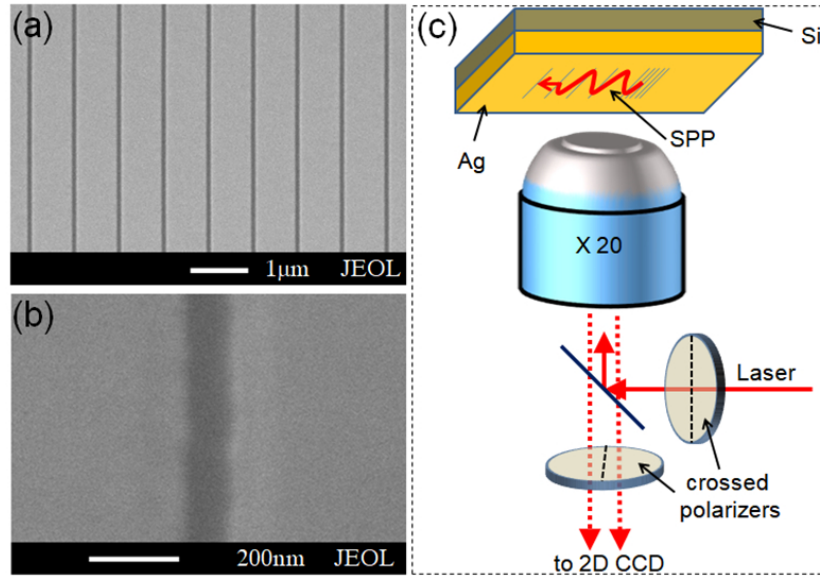


Fig. 1. (a) an electron microscope image of nanoslits array on the Ag film used to excite SPP, (b) an electron microscope image of a nanogroove used to detect SPP, (c) a schematic diagram of the experimental set up.

detected radiation are orthogonal, which makes it possible to reduce parasitic scattered radiation (from the reflected and scattered laser light on the sample).

Fig.2(a) shows the Ag film surface optical image with fabricated nanostructures on it that were made by an ion-beam lithography. The figure clearly shows both types of nanostructures. One is the array of nanoslits, designed to excite the SPP and which is visible as a rectangle. The distance between nanoslits is too small to be resolved by optical microscope. The figure also clearly shows distinctly separated nanogrooves. These nanogrooves are arranged parallel to the nanoslits and are on the way of the SPP propagation. Scattering of the SPP on each nanogroove allows us to visualize the SPP, and also to measure the SPP propagation length.

Figure 2b shows an optical image of the silver thin film when it is irradiated by laser radiation at wavelength 780 nm. As can be seen from the figure, a strong scattering of laser radiation on the array of nanoslits and the excitation of SPP on the Ag film surface appear. The SPP propagates and scatters on nanogrooves, giving possibility to visualize SPP propagation in optical microscope. Each of the spot on a nanogroove has elliptical shape. The smaller diameter d_1 of this spot is determined by a diffraction limit of used optical objective. The larger diameter of the spot d_2 is determined by width of SPP. Thus the optical image clearly shows the divergence of the SPP due to diffraction: as the distance from the excitation region of the SPP wave increases, the spot diameter d_2 (from the scattering of the SPP wave by the nanogrooves) becomes higher. This spot size on a nanogroove located close to the array of nanoslit is $d_2(0 \mu\text{m}) = 6 \mu\text{m}$ and corresponds to the diameter of the exciting laser beam. On the nanogroove located at $L = 275 \mu\text{m}$ from the first nanogroove, the corresponding spot size is much larger: $d_2(275 \mu\text{m}) = 38 \mu\text{m}$.

Fig.2(c) shows a cut image of Fig.2(b) along the SPP propagation direction. As can be seen from the Fig.2(b), the scattering signals from the nanogrooves are represented by the narrow peaks with a width equal to $d_1 = 2 \mu\text{m}$, which is determined by the resolution of the objective lens with a numerical aperture $NA = 0.4$ ($d_1 \approx \lambda/NA$).

It can be seen from Fig.2(b,c) that the amplitudes of the scattering signal of SPP on the grooves decrease with increasing distance between the nanogroove and the array of nanoslits because of

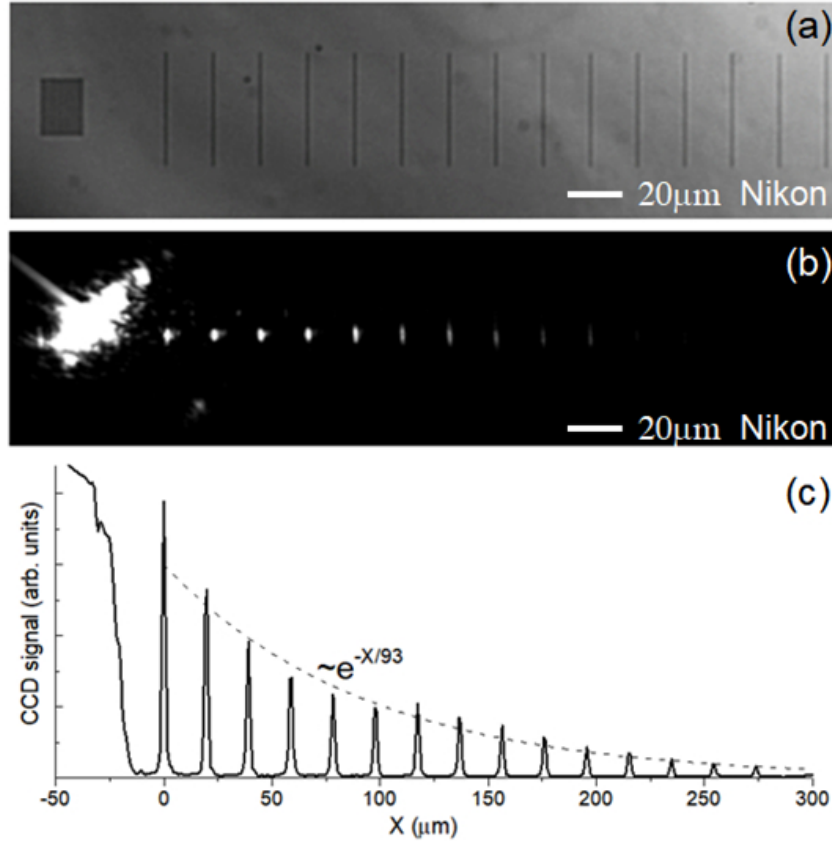


Fig. 2. Optical microscopy of SPP: (a) optical image of an Ag film surface with nanostructures created by a focused-ion-beam lithography, (b) optical image of Ag film surface when SPP is excited by a laser radiation, (c) the cut image of Fig.2(b) along the SPP propagation direction; the dotted curve - the approximation by exponential curve with the characteristic decay length of 93 μm .

the losses of the SPP in Ag thin film. The change in the amplitudes is well approximated by an exponential curve with a characteristic length equal to 93 μm . This measured SPP decay length is determined by three factors: (1) absorption losses of the SPP in the silver film, (2) losses of the SPP due to scattering on each nanogroove, and (3) divergence of the SPP wave caused by its diffraction. We will show below that from these measurements it is possible to determine the SPP propagation length determined only by the losses in the silver film.

Using the method described in [16], we measured losses of a SPP on each nanogroove, which equals to 4.8%. The SPP diffraction was taken into account by integrating the signal along the nanogroove, using the image of Fig.2(b), which corresponds to scattering of the SPP by the nanogroove. Fig.3 shows the dependence of the attenuation of the intensity of the SPP, taking into account the losses at each nanogroove and taking into account the diffraction of the SPP wave. As can be seen from the figure, the data are well approximated by an exponential curve with an attenuation length characterizing SPP propagation length on a surface of Ag nanofilm $L_{SPP} = 194 \pm 23 \mu\text{m}$. In this figure, the zero position on the x axis corresponds to the edge of the nanoslits array (used to excite the SPP). It is also seen from the figure that even at a distance of 300 μm from the excitation region, the SPP still has contained a significant amount of energy to be easily detected.

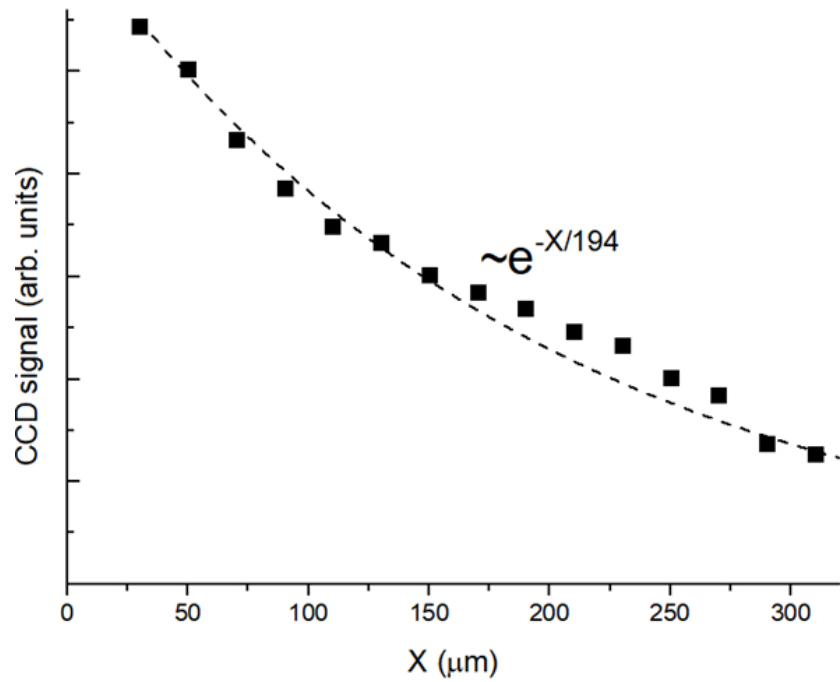


Fig. 3. The decay curve of the SPP on an Ag thin film surface.

4. Conclusion

Thus, we demonstrated the SPP propagation on the Ag film surface with a record length of propagation $L_{SPP} = 194 \mu\text{m}$ that is two times longer than previously reported. The measured SPP propagation length corresponds to the calculated data, in which the optical constants of the silver film are taken from [15]. The carried out measurements convincingly show the extremely high quality of the silver films created by the new method (SCULL process, to be published). This opens up new horizons in the development elements of nanoplasmonics, based on the use of silver films having low losses.

Acknowledgments

Silver film samples were made at the BMSTU Nanofabrication Facility (Functional Micro/Nanosystems, FMNS REC, ID 74300). This work was performed using equipment of MIPT Shared Facilities Center and with financial support from the Ministry of Education and Science of the Russian Federation (Grant No. RFMEFI59417X0014)